metals

MDPI

Article

The Role of Mechanical Connection during Friction Stir Keyholeless Spot Welding Joints of Dissimilar Materials

Xiao Liu [1], Xijing Wang [1,2,*], Boshi Wang [1], Liangliang Zhang [1], Chao Yang [1] and Tingxi Chai [1]

[1] State Key Laboratory of Advanced Processing and Recycling of Non-Ferrous Metals, Lanzhou University of Technology, Lanzhou 730050, China; 18119316859@163.com (X.L.); tianyjs_1988@163.com (B.W.); zll_0715@126.com (L.Z.); tijs_1988@126.com (C.Y.); 18509316693@163.com (T.C.)

[2] School of Materials Science and Engineering, Lanzhou University of Technology, Lanzhou 730050, China

* Correspondence: wangxj@lut.cn; Tel.: +86-133-2122-2432

Academic Editor: Giuseppe Casalino

Received: 9 May 2017; Accepted: 5 June 2017; Published: 13 June 2017

Abstract: Contrast experiments of lap joints among dissimilar AZ31B Mg alloy, Mg99.50, zinc-coated DP600 sheet, and non-zinc-coated DP600 sheet were made by friction stir keyholeless spot welding (FSKSW) and vacuum diffusion welding (VDW), respectively. Scanning electron microscopy (SEM) and energy disperse spectroscopy (EDS) were used to investigate the microstructures and components of the joints welded. The experimental results show that the FSKSW bonding method is a kind of compound mode that contains a mechanical connection and element diffusion fusion connection, in which mechanical connection has the main decisive function on joints of Mg/steel. Elements diffusion exists in the interfacial region of the joints and the elements diffusion extent is basically the same to that of VDW. The elements' diffusion in Mg/steel using FSKSW is defined in the reaction between small amounts elements of the base metal and zinc-coated metals. The intermetallic compounds and composite oxide perform some reinforcement on the mechanical connection strength.

Keywords: friction stir keyholeless welding; magnesium alloy; duplex steel 600; compound joints; mechanical connection; dissimilar materials

1. Introduction

Magnesium (Mg) alloy has a higher strength to weight ratio, is one of the lightest alloys in modern industrial applications [1]. Mg alloys can conform to the requirements of automotive technology development with reducing vehicle weight, lowering emissions, improving fuel economy, and other aspects. So many countries have begun to try using Mg alloys in automotive manufacturing [2,3]. Duplex steel 600 (DP600) has high strength and high formability, especially for the manufacture of automotive bodies. With the further expansion applications of Mg alloys and intersection applications between Mg alloys and steel, composite structures can replace steel structures, effectively reducing the weight of structural parts, solving the problem of light-duty trends in the transport industry and further providing feasible technical support for energy saving and environmental protection. Therefore, the welding of Mg and steel has been widely concerned by many scholars [4–8]. Some well-known automotive companies, such as Japan Mazda and General Motors, try to apply the above technology to the welding of Mg alloy and steel in automotive manufacturing. However, this technology has not been applied to actual production due to the difficulty of welding and the lack of exploration of the joint connection mechanism [9].

For dissimilar metal welding of Mg/steel, resistance spot welding, laser welding-brazing, composite heat tungsten inert gas welding, and diffusion welding are mainly adopted by many researchers, in which

laser welding has been widely used in joining dissimilar metals. Casalino et al. [10] found that a fiber laser was used to perform a dissimilar metal joining between AZ31B Mg and 316 stainless steel with the ultimate tensile strength exceeding 100 MPa. Rossini et al. [11] conducted experiments with dissimilar joints between the DP, hotstampingboron (22MnB5) steels, and TRansformation Induced Plasticity (TRIP) steels with exhibiting good resistance properties. However, due to the very large differences in the physical properties of Mg and steel, and poor interactions, conventional processes have exhibited some disadvantages, such as a large heat-affected zone (HAZ), solidification cracking, porosity, evaporative loss of the alloying elements, and high residual stresses resulting in low welding joint strength [12,13]. After consulting a large volume of literature, the lap joints of Mg–steel obtained by fusion welding methods have maximum shear loads of 5 kN [14] (resistance spot welding) and the minimum value of 767 N (laser welding-brazing) [15].

Friction stir welding (FSW) is an alternative method with lower residual stress and less distortion, which could overcome the above disadvantages, since FSW is performed below the melting temperature of the material to be welded, and it produces pore-free joints and smaller temperature gradients than conventional fusion welding [16]. There are many advantages of overcoming large differences of dissimilar material properties and it is found that FSW is an ideal method of connecting dissimilar materials. Xu et al. [17] studied the strength of pinless friction stir spot welding joint with addition of a thin Zn interlayer, and the results showed that an intermetallic layer was formed due to an alloying reaction occurring between the Mg substrate and Zn interlayer during friction stir spot welding (FSSW). Chen et al. [18,19] obtained a high strength connection joint with a lap configuration of setting Mg on top of steel by FSW. Our research group has obtained a certain strength connection joint with a lap configuration of setting steel on top of Mg by FSW and the lap shear tensile test results reach the highest value (9.98–11.75 kN), which is higher than most of joints welded by other methods. Thus, this method has the prospect of practical application.

In this paper, we respectively carry out lap welding experiments with AZ31B Mg alloy, Mg99.50, DP600, and non-zinc-coated DP600 by using friction stir keyholeless spot welding (FSKSW). Comparing the mechanical properties of those joints and using scanning electron microscopy (SEM) and energy disperse spectroscopy (EDS), we investigate the microstructure and the distribution of elements in the stir zone in order to concretely analyze the bonding method of Mg/steel joints, and the reason why the joint strength of FSKSW is higher than other welding methods is further explained.

2. Materials and Methods

2.1. Materials

AZ31B Mg alloy and Mg99.50 with a thickness of 2.0 mm, and DP600 and non-zinc-coated duplex steel polished to remove the zinc layer of DP600 with a thickness of 1 mm, were welded in this study. The chemical compositions of these materials are listed in Tables 1 and 2, respectively.

Table 1. Chemical compositions of AZ31B and Mg99.50 (in wt %).

Alloys	Al	Zn	Mn	Si	Fe	Cu	Ni	Mg
AZ31B	2.5–3.5	0.6–1.4	0.2–1.0	0.80	0.003	0.01	0.001	Balance
Mg99.50	-	-	-	-	-	-	-	≥99.50

Table 2. Chemical compositions of zinc coated * duplex steel (in wt %).

C	Si	Mn	P	S	Al	N	Fe
0.079	1.00	1.52	0.015	0.005	0.023	0.0037	Balance

* The thickness of zinc coated is 15–20 μm.

The reasons for selecting above four kinds of material are as follows: firstly, AZ31B Mg alloy and DP600 are commonly used in automotive manufacturing with their practical application values; secondly, Mg99.50 contains nearly no other elements; thirdly, compared with AZ31B Mg alloy, Mg99.50 can exclude the effect of Al, Zn, and other elements for the joint bonding degree and, compared with DP600, non-zinc-coated duplex steel can exclude the effect of the 15–20 μm zinc layer for the joint bonding degree.

2.2. Methods

Conventional friction stir spot welding has its own disadvantages with being conducive to the material flow and smaller solder joint, the mechanical properties of welded joints were reduced. Thus, the keyholeless spot welding utilized in this experiment was self-designed by our research group. Figure 1 shows the new keyholeless spot welding, whose basic principles are the same as the traditional process and the keyholeless joints were obtained through the relative movements between the tool and tool shoulder. Whereas the retraction of the tool with the simultaneous move distance of the half shoulder diameter of the shoulder can increase the solder joint area of enhancing bonding strength with smooth formation. At the same time, the moving retraction made the relative flow degree of parent material more intense to achieve a reliable composite of the joint [20–22].

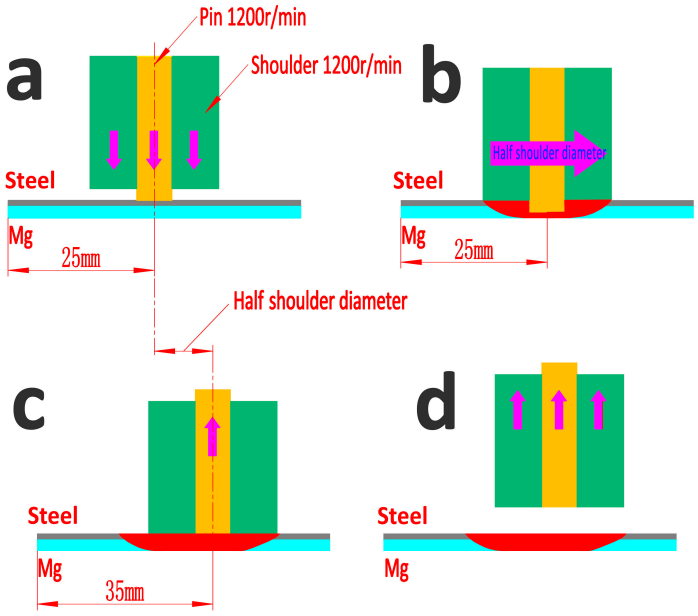

Figure 1. The diagram of new keyholeless spot welding: (**a**) The start of welding; (**b**) the welding process with the retraction of the pin; (**c**) the finished retraction; and (**d**) the end of welding.

The dimension of the specimens was 150 mm in length and 50 mm in width. A lot of experiments have found that the Mg plate would appear black, even burning, owing to serious oxidation, especially when the Mg plate was placed on the top of the steel. At the same time, considering the large difference of the melting point between Mg and steel, the materials directly contacting with the shoulder should choose the high melting point metal to ensure the utilization rate of heat generated by the rotating shoulder. Thus, all welds were made in a lap joint configuration with AZ31B on the bottom and DP600 on the top, as shown in Figure 2.

In this experiment the optimal process parameters, referred to the research results of other process parameters and combined with the experimental homework [23–26], were as follows: the diameter of the tool is 6.0 mm; the rotation speed of the tool is 1200 r/min; the diameter of the tool shoulder is 22 mm and the vertical descent of the shoulder is 0.2 mm [27].

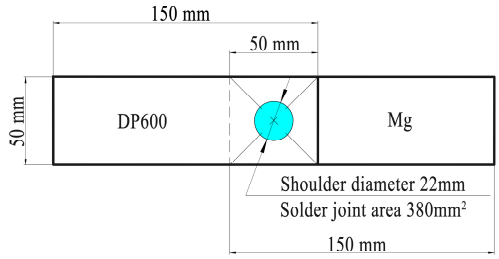

Figure 2. The lap joint diagram of friction stir keyholeless spot welding (FSKSW).

During the dissimilar material FSKSW process, intermetallic compounds were formed by element diffusion [28,29]. The material in thermo-mechanically affected zone (TMAZ) near the surface of the weld transfers downwards, and the material in the middle of weld moves upward, as a result of formation mechanical connection [30]. Compared with FSKSW, the VDW is a solid diffusion process of pure element that could eliminate the interference of other factors in welding. FSKSW joints with coupling the element diffusion and mechanical connection, the VDW could gain the most typical solid diffusion joints that are more comparable and representative than FSSW.

In order to compare the mechanical properties of welded joints, the joint area of the vacuum diffusion welding (VDW) should be the same as FSKSW. Thus, the dimension of the specimens was 70 mm in length and 19.5 mm in width. The optimum process parameters were chosen after many experiments and they were as follows: diffusion pressure was 10 MPa and the heating temperature was 450 °C with a holding time of 1 h. Then natural cooling of the joints was conducted in a furnace with the vacuum degree kept unchanged. The lap configuration is shown in Figure 3.

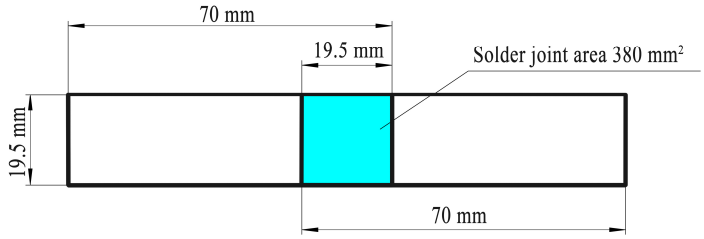

Figure 3. The lap joint diagram of vacuum diffusion welding (VDW).

After the welding test, the mechanical properties of the welded joints are studied using a universal material testing machine (Jinan MTS Test Technology Co., Ltd, Jinan, China) with a strain rate of 0.0025 s^{-1} at room temperature. Along the travel direction of the tool, the transverse weld cross-section samples were cut out and polished in order to observe the microstructure and the element distribution of those joints via SEM (FEI, Hillsboro, OR, USA) and EDS (Oxoford instruments, Oxoford, UK). Then we further clarified the bonding method of the Mg/steel welded by FSKSW and the effect of the mechanical connection on those welding joints was analyzed.

3. Results

3.1. Joint Formation

Figure 4 shows FSKSW joints of the combination of four materials. The morphology of the welding is smooth and neat in the welding region center. Thus, joints welded were visually inspected for good shape and no scrap. Due to the high temperature in the welding process, the surrounding of joints were oxidized with appearing black color of individual joints. Compared with the surrounding of the joints, the center of the stir zone was not oxidized under the protection of the shoulder and appeared with a metallic luster.

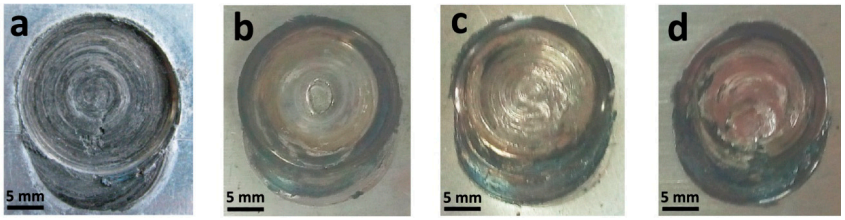

Figure 4. Solder joint appearance of FSKSW: (**a**) AZ31/DP600; (**b**) AZ31/non-zinc-coated DP600; (**c**) Mg/DP600; (**d**) Mg/non-zinc-coated DP600.

Figure 5 shows VDW joints of the combination of four materials. Under the effect of pressure, the Mg alloy had slight deformation. In label B of the Figure 5a,c, the outer zinc of DP600 was melted down and the joints were filled owing to the wetting of the melting zinc. Subsequently, the joints were formed by the diffusion process between the liquid phase and the solid phase under the heat holding process. However, as shown in the Figure 5b,d, there was no wetting phenomenon owing to the polished zinc coating of DP600.

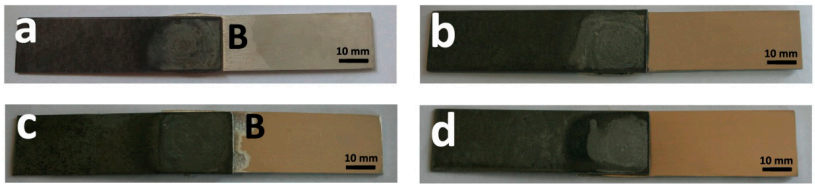

Figure 5. Solder joint appearance of VDW: (**a**) AZ31/DP600; (**b**) AZ31/non-zinc-coated DP600; (**c**) Mg/DP600; (**d**) Mg/non-zinc-coated DP600.

3.2. Macro-Organization Characteristics

Figure 6 shows transverse cross-section morphology of the combination of four materials. As shown in Figure 6, we can obviously conclude that Mg/steel welding joints had the typical feature of mechanical connection with a serrated bonding interface no matter what types the joints were. It was showed that the base material attained a thermoplastic state under the drastic and fast rotation of the tool and shoulder. Mg/steel components were intermixed together and the bonding interface was changed from the linear shape to the curved shape. As shown in label A and B of Figure 6, the steel components that were stirred into the Mg matrix was similar to the rivet or hook embedded in the Mg and further formed a solid joint.

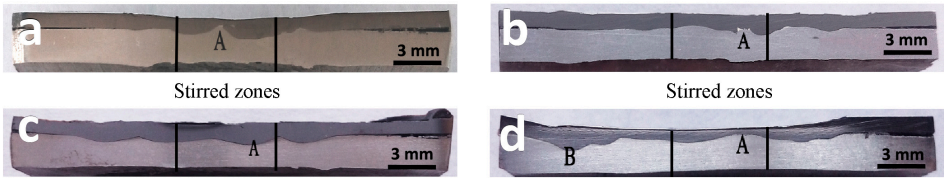

Figure 6. Weld cross-section morphology of FSKSW: (**a**) AZ31/DP600; (**b**) AZ31/non-zinc-coated DP600; (**c**) Mg/DP600; (**d**) Mg/non-zinc-coated DP600.

Figure 7 shows VDW joints of the combination of three materials. Owing to having no bonding strength between Mg99.50 and non-zinc-coated DP600, the joint had separated in the cutting of the metallographic samples. Therefore, the weld morphology was not listed in Figure 6. As shown in label A of Figure 6, and C, D, and E of the Figure 7, the interface of Mg/steel was smooth and there is no

deformation. The interface of Mg/steel only depended on the solid phase diffusion mechanism to form the effective bonding.

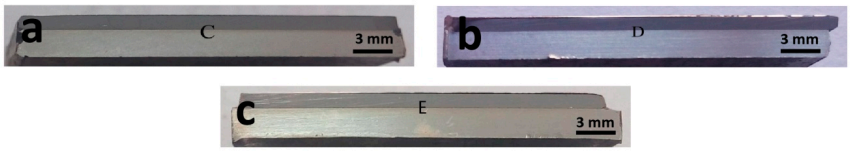

Figure 7. Weld cross-section morphology of VDW. (**a**) AZ31/DP600; (**b**) AZ31/ non-zinc-coated DP600; (**c**) Mg/DP600.

3.3. Degree of Elements Diffusion Analysis of the Joint

To compare and investigate the degree of elements diffusion in the joint interface between FSKSW and VDW, some experiments were performed using EDS in the joint interface shown in label A of Figure 6 and in label C, D, and E of Figure 7, respectively, and conclusions were shown in Figure 8, which shows distribution charts and percentages of the joint elements.

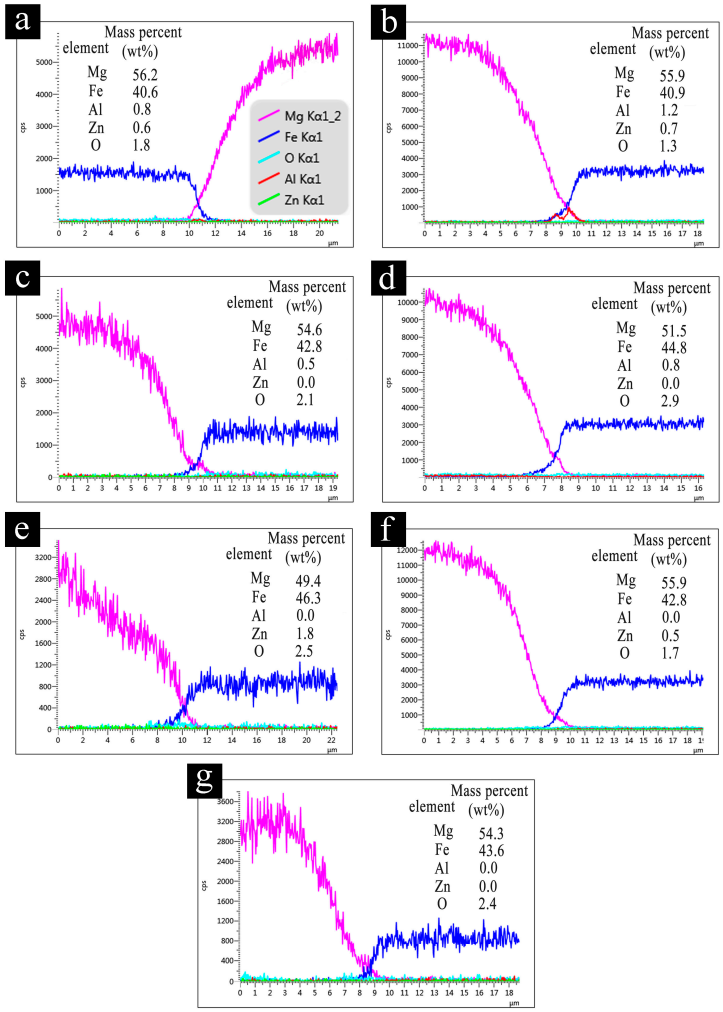

Figure 8. The analysis of a line scan by energy dispersive spectroscopy (EDS) experimentation using two methods in four materials: (**a**) FSKSW AZ31/DP600; (**b**) VDW AZ31/DP600; (**c**) FSKSW AZ31/non-zinc-coated DP600; (**d**) VDW AZ31/non-zinc-coated DP600; (**e**) FSKSW Mg99.50/DP600; (**f**) VDW Mg99.50/DP600; and (**g**) FSKSW Mg99.50/non-zinc-coated DP600.

It can be concluded that the Mg/steel surface in FSKSW and VDW mainly contains Mg, Fe, Al, Zn, and O. These five elements, with the spectral line of Mg and Fe, interacted each other. The result means that Mg and Fe barely have any solid solubility. However, no matter the kinds of joints, all joint regions have the situation that Mg and Fe in the bonding interface diffuse mutually during the welding process. Additionally, we can obviously figure out in Figure 8a–g that the spectral line's staggered width of Mg and Fe is around 2 μm, meaning that although the method of welding is different, the extent of diffusion in Mg and Fe had no difference and the percentage of the joint regions had little distinction. The content of trace elements, such as Zn, Al, and coated metal, are low, which is not obvious in the spectral line and indicated in the percentage of contents in the joint zone. As is shown in Figure 8c,d, as for DP600 the zinc layer has been polished away and the content of Zn in AZ31B is rather low, Zn can hardly be detected. As no Al can be detected in Mg99.50 and DP600, the mass percent of Al in Figure 8e–g is zero. O can be detected in both samples owing to the oxidation of Mg in the process of making samples. The zinc layer thickness of DP600 is about 15–20 μm and, according to theory, it should be found that relatively higher content of Zn exists in DP600 joints. However, owing to the high temperature leading to the evaporation loss of Zn, the content of Zn is relatively lower in joints. Since Mg99.50/non-zinc-coated DP600 has no bonding strength, meaning samples cannot be made, so there is no picture to analyze.

3.4. Phase Analysis of Joints

Further analysis of phase in the Mg interface with X-ray Diffraction (XRD), is shown in Figure 9.

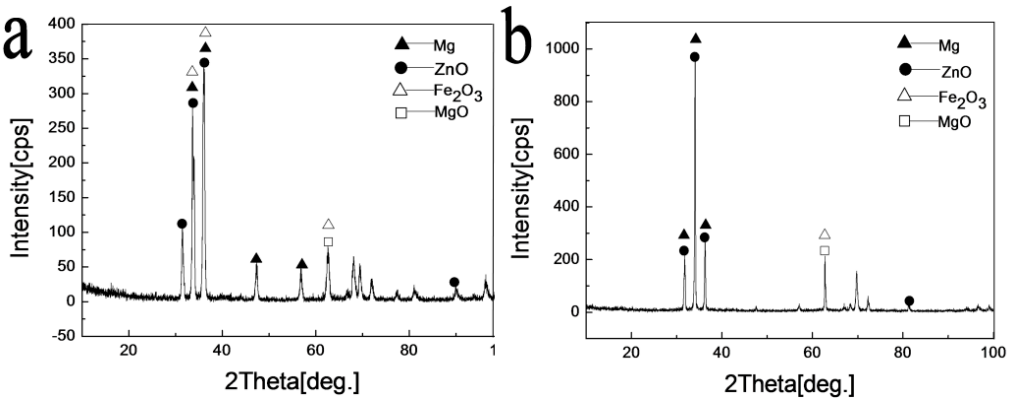

Figure 9. The analysis of X-ray Diffraction (XRD) experimentation using two methods: (**a**) Mg99.50/DP600 FSKSW; and (**b**) Mg99.50/DP600 VDW.

Figure 9a,b shows the result of the Mg99.50/DP600 using FSKSW and VDW, respectively. It can be indicated that the bonding surface using FSKSW mainly contains the intermetallic compounds including Mg, ZnO, Fe_2O_3, and MgO may exist. However, the bonding surface using VDW mainly contains Mg, ZnO, and Fe_2O_3 and MgO may exist.

3.5. Mechanical Properties Comparison and Analysis

The mechanical properties of samples were performed using a universal WDW–100E material testing machine (Jinan MTS Test Technology Co., Ltd, Jinan, China) and the results are showed in Table 3.

Table 3. Shear tensile properties of samples (kN).

Joint Type	Joint 1	Joint 2	Joint 3	Average
AZ31B–DP600 FSKSW	9.98	11.75	10.36	10.36
AZ31B–DP600 VDW	3.35	3.02	2.86	3.07
AZ31B–non-zinc-coated DP600 FSKSW	11	9.4	9.1	9.83
AZ31B–non-zinc-coated DP600 VDW	1.575	1.8	2.225	1.87
Mg99.50–DP600 FSKSW	7.2	10.2	7.8	8.4
Mg99.50–DP600 VDW	2.2	2.3	3.8	2.77
Mg99.50–non-zinc-coated DP600 FSKSW	3.14	6.9	5.3	5.11
Mg99.50–non-zinc-coated DP600 VDW	0.55	0.8	0.5	0.61

The regular rule of lap shear tensile test results can be concluded from the table above. Distinguished from the welding methods: FSKSW > VDW; distinguished from the material combination: FSKSW AZ31B–DP600 > AZ31B–non-zinc-coated DP600 > Mg99.50–DP600 > Mg99.50–non-zinc-coated DP600. However, VDW AZ31B–DP600 > Mg99.50–DP600 > AZ31B–non-zinc-coated DP600 > Mg99.50–non-zinc-coated DP600. Data is plotted in a histogram and shown in Figure 10.

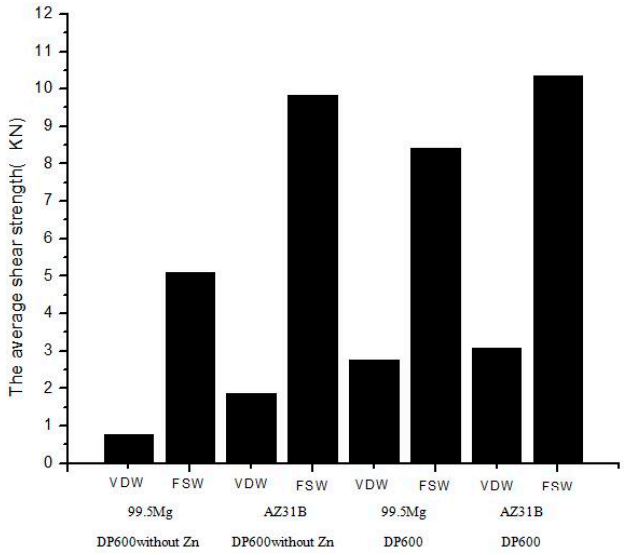

Figure 10. The histogram of tensile properties of samples.

As is shown in Figure 10, the load of the lap shear tensile test on different material combinations using FSKSW is much higher than the joint of using VDW and the average numerical difference is around 7.96 to 4.5 kN.

The analysis from different material combinations shows that elements in AZ31B/DP600 are much greater than others, and the thickness of the zinc layer of DP600 is about 15–20 μm, which is conducive to the formation of high-strength joints, so it has the highest strength to resist shear tensile force no matter if FSKSW or VDW is applied. As most of the zinc layer has been extruded by the shoulder when using FSKSW, leading to fewer metal compounds, and also means Zn has little effect in the FSKSW process. However, when using VDW, the wetting spreadability of Mg in iron can be obviously enhanced by Zn, which plays an important role in the formation of joints. Thus, the load of lap shear tensile tests on samples using FSKSW is shown: AZ31B/non-zinc-coated DP600 > Mg99.50/DP600, while using VDW Mg99.50/DP600 > AZ31B/non-zinc-coated DP600. The joint of Mg99.50/non-zinc-coated DP600 barely has any other metal compounds except for a very small content of Al (0.023%) in DP600, so it has the lowest strength to resist shear tensile force either in FSKSW or VDW, and has no connection strength in VDW.

3.6. Analysis of the Effect of Mechanical Connection

It can be concluded from the diffusion extent of joint elements (Section 3.3) and the phase analysis of joint (Section 3.4) that diffusion extent (Mg, Fe) of joints on different combinations can be basically consistent no matter whether FSKSW or VDW (about 2 μm) methods are used, and the phase analysis has no obvious difference, which mean the mechanical properties of these two methods of welding are almost equal if other bonding modes are not taken into consideration. However, the average load of lap shear tensile tests in joints using FSKSW can be three times higher than using VDW. The joint of Mg99.50/non-zinc-coated DP600 barely has any other alloy elements; as for the no solid solubility between Mg and Fe, the joints of VDW have no connection strength making it difficult for sample preparation. However, the joint of Mg99.50/non-zinc-coated DP600 using FSKSW still has an average lap shear tensile force (5.11 kN) that is even higher than the highest lap shear tensile force (2.04 kN) of the AZ31B/DP600 joint using VDW. Experimental results seem contrary to common sense. The reason for this situation results from the special connection method of FSKSW: mechanical connection.

Figure 11 shows the typical mechanical connection structure of FSKSW. During welding process, the effect of the process of intense rotation and extruding by the tool and the shoulder makes the Mg into thermoplastic flowing state. However owing to the welding parameters being taken into consideration to prevent the evaporation loss of Mg, the heat is too low to turn iron into a thermoplastic state. The iron, with half thermoplastic state, can emerge local plastic flow and irregular deformation even tearing with the drive of the tool and the extrusion of the shoulder, at the meantime, thermoplastic Mg flows into voids or gap resulting from of the iron deformation under the process of welding. The shape of hook-like, as shown in Figure 11 zigzag interface A, B and C or convex in shape, is emerging with the form being similar to the zigzag connection interface of the explosion welding joints, which can ensure the reliability of the joint connection.

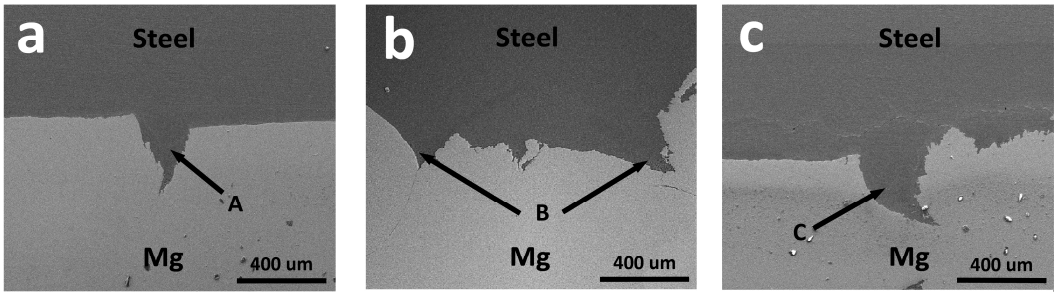

Figure 11. The typical mechanical connection of FSKSW: (**a**) zigzag interface A; (**b**) zigzag interface B; and (**c**) zigzag interface C.

It is the effective connection of mechanical way that makes the bonding way the decisive factor to the metallurgical reactions of alloy elements with FSKSW which can explain that there is no connection strength in Mg99.50/non-zinc-coated DP600 joint with VDW, while the joint of FSKSW still has shear tensile force (5.11 kN). It can be further confirmed in the macro-morphology of the tensile fracture surface in Figure 12.

As is shown in Figure 12A, the fractography of the failed interface was carried out to investigate the tear morphology and hole no matter in the side of iron or Mg, which is aroused by the physical connection of iron and Mg.

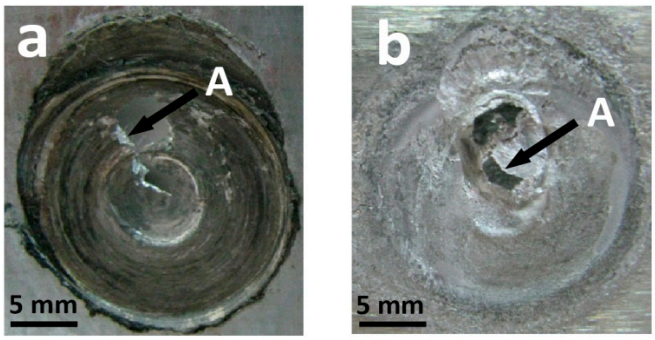

Figure 12. The macro-morphology of tensile fracture surface: (**a**) side of iron; (**b**) side of Mg.

Although the main bonding way of FSKSW in Mg/steel is mechanical connection, it can be concluded from the histogram of tensile properties of samples shown in Figure 10 that the composition of the different alloy elements still affect the strength of joints. In other words, the intermetallic compounds and composite oxides enhance the strength of mechanical connection and whether enhancement effect is linear or not still needs further validation and research. The mechanical connection and diffusion connection of different material combinations of the load shear tensile ratio is shown in Figure 13. The red region means mechanical connection while the black region means diffusion combination.

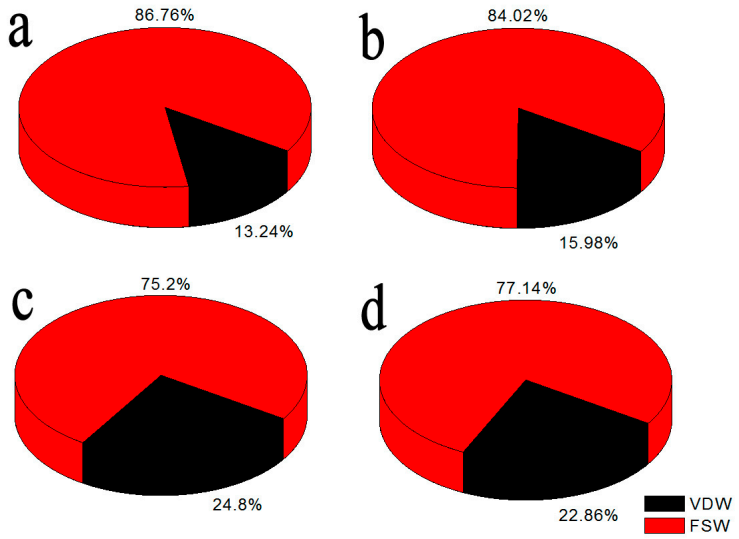

Figure 13. The proportion of joint shear force: (**a**) Mg99.50/non-zinc-coated DP600; (**b**) AZ31/non-zinc-coated DP600; (**c**) Mg99.50/DP600; and (**d**) AZ31/DP600.

It is obvious that in Figure 13 the proportion of mechanical connection in joints using FSKSW stands 75.2–86.76%, in which the diffusion connection proportion of joints with having DP600 stands 22.86–24.8% that is higher than the diffusion connection proportion of joints with non-zinc-coated DP600 (13.24–15.98%), and it can make sure that the Zn element plays an important role in metallurgical bonding method of Mg/steel which conforms to the conclusion made by other methods of welding. The joints of Mg99.50/non-zinc-coated DP600 barely have any other intermetallic compounds or composite oxides, leading to the highest proportion of mechanical connection.

4. Conclusions

Contrast experiments of lap joints among dissimilar AZ31B Mg alloy, Mg99.50, zinc-coated DP600 sheet, and non-zinc-coated DP600 sheet were made by FSKSW and vacuum diffusion welding. The main findings can be concluded as follows:

The FSKSW bonding method is a type of compound mode which contains mechanical connection and element diffusion fusion connection.

Mechanical connection is the main decisive function on joints of Mg/steel using FSKSW, in which the connection strength withstands the whole strength by 75.2–86.76%.

The elements diffusion in Mg/steel using FSKSW is defined in the reaction between small amounts of elements of the base metal and zinc-coated metals, and a certain amounts of the intermetallic compounds and composite oxide can perform auxiliary reinforcement on the mechanical connection strength to some extent.

Acknowledgments: This work was supported by major national science and technology projects under No. 2012ZX04008011 and the fundamental research funds of Gansu province for higher education institutions.

Author Contributions: Xiao Liu did the experiment, data analysis and wrote the paper. Xijing Wang reviewed and revised the manuscript of this paper. Boshi Wang, Liangliang Zhang, Chao Yang and Tingxi Chai contributed to the data analysis.

Conflicts of Interest: The authors declare no conflicts of interest.

References

1. Zeng, R.; Wei, K.E.; Yongbo, X.U.; Han, E.; Zhu, Z. Recent development and application of magnesium alloys. *Acta Metall. Sin.* **2001**, *37*, 672–685.
2. Sato, Y.S.; Park, S.H.C.; Michiuchi, M.; Kokawa, H. Constitutional liquation during dissimilar friction stir welding of Al and Mg alloys. *Scr. Mater.* **2004**, *50*, 1233–1236. [CrossRef]
3. Somasekharan, A.C.; Murr, L.E. Microstructures in friction-stir welded dissimilar magnesium alloys and magnesium alloys to 6061–T6 aluminum alloy. *Mater. Charact.* **2004**, *52*, 49–64. [CrossRef]
4. Marya, M.; Edwardz, G.R. Chloride contributions in flusassisted GTA welding of magnesium alloys. *Weld. J.* **2002**, *81*, 291–298.
5. Zhang, Z.D.; Liu, L.M.; Wang, L. Microstructure feature analysis of activating TIG welded joint. *Trans. China Weld. Inst.* **2004**, *25*, 55–58.
6. Mayer, A.; Isakovic, J.T.; Zhuang, H.S. Friction stir spot welding. *Weld. Join.* **2009**, *9*, 6–10.
7. Liu, H.J.; Liu, C.; Shen, J.J.; Liu, Y.Z. Progress in friction stir welding of aluminum to copper. *Weld. Join.* **2009**, *9*, 11–15.
8. Dong, T.; Wang, L.; Lu, C.J.; Wang, M. Study progress of friction stir spot welding at home and abroad. *Mod. Weld. Technol.* **2012**, *2*, 1–4.
9. Fujimoto, M.; Inuzuka, M.; Koga, S. Development of friction spot joining. *Weld. World* **2005**, *49*, 18–21. [CrossRef]
10. Casalinoa, G.; Guglielmia, P.; Lorussoa, V.D.; Mortellob, M.; Peyrec, P.; Sorgenteda, D. Laser offset welding of AZ31B magnesium alloy to 316 stainless steel. *J. Mater. Process. Technol.* **2017**, *242*, 49–59. [CrossRef]
11. Rossini, M.; Spena, P.R.; Cortese, L.; Matteis, P.; Firrao, D. Investigation on dissimilar laser welding of advanced high strength steel sheets for the automotive industry. *Mater. Sci. Eng. A* **2015**, *628*, 288–296. [CrossRef]
12. Thomas, W.; Nicholas, E.D.; Staines, D.; Tubby, P.J.; Gittos, M.F. FSW process variants and mechanical properties. *Weld. World* **2005**, *49*, 4–11. [CrossRef]
13. Lee, C.Y.; Lee, W.B.; Kim, J.W.; Choi, D.H.; Yeon, Y.M.; Jung, S.B. Lap joint properties of FSWed dissimilar formed 5052 Al and 6061 Al alloys with different thickness. *J. Mater. Sci.* **2008**, *43*, 3296–3304. [CrossRef]
14. Nasiri, A.M.; Weckman, D.C.; Zhou, Y. Interfacial Microstructure of Diode Laser Brazed AZ31B Mg to Steel Using a Nickel Interlayer. *Weld. J.* **2013**, *92*, 1–10.
15. Liu, L.; Xiao, L.; Feng, J.C.; Tian, Y.H.; Zhou, S.Q.; Zhou, Y. The Mechanisms of Resistance Spot Welding of Magnesium to Steel. *Metall. Mater. Trans. A* **2010**, *41*, 2651–2661. [CrossRef]

16. Mohammadi, J.; Behnamian, Y.; Mostafaei, A.; Izadi, H.; Saeid, T.; Kokabi, A.H.; Gerlich, A.P. Friction stir welding joint of dissimilar materials between AZ31B magnesium and 6061 aluminum alloys: Microstructure studies and mechanical characterizations. *Mater. Charact.* **2015**, *101*, 189–207. [CrossRef]
17. Xu, R.Z.; Ni, D.R.; Yang, Q.; Liu, C.Z.; Ma, Z.Y. Pinless friction stir spot welding of Mg–3Al–1Zn alloy with Zn interlayer. *J. Mater. Sci. Technol.* **2016**, *32*, 76–88. [CrossRef]
18. Chen, Y.C.; Nakata, K. Effect of surface states of steel on microstructure and mechanical properties of lap joints of magnesium alloy and steel by friction stir welding. *Sci. Technol. Weld. Join.* **2013**, *15*, 293–298. [CrossRef]
19. Chen, Y.C.; Nakata, K. Effect of tool geometry on microstructure and mechanical properties of friction stir lap welded magnesium alloy and steel. *Mater. Des.* **2009**, *30*, 3913–3919. [CrossRef]
20. Wang, X.; Zhang, Y.; Zhang, Z.; Sun, X. Welding analyses of friction stir spot welding without keyhole between aluminum alloy and zinc-coated steel. *Trans. China Weld. Inst.* **2015**, *36*, 1–4.
21. Wang, X.J.; Li, W.H.; Zhao, G. Process analysis on friction stir spot welding without keyhole between magnesium and steel dissimilar alloys. *Trans. China Weld. Inst.* **2014**, *35*, 23–26.
22. Paradiso, V.; Astarita, A.; Carrino, L.; Durante, M.; Franchitti, S.; Scherillo, F.; Squillace, A.; Velotti, C. Numerical optimization of selective superplastic forming of friction stir processed AZ31 Mg alloy. *Key Eng. Mater.* **2013**, *554–557*, 2212–2220. [CrossRef]
23. Carrino, L.; Squillace, A.; Paradiso, V.; Ciliberto, S.; Montuori, M. Superplastic forming of friction stir processed magnesium alloys for aeronautical applications: A modeling approach. *Mater. Sci. Forum* **2013**, *735*, 180–191. [CrossRef]
24. Shen, Z.; Chen, Y.; Haghshenas, M.; Gerlich, A.P. Role of welding parameters on interfacial bonding in dissimilar steel/aluminum friction stir welds. *Eng. Sci. Technol. Int. J.* **2015**, *18*, 270–277. [CrossRef]
25. Chiteka, K. Friction Stir Welding of steels: A Review Paper. *J. Mech. Civ. Eng.* **2013**, *9*, 16–20.
26. Wang, X.; Zhao, G.; Zhang, Z.; Wang, P. Process research on friction stir spot welding without key hole between magnesium and steel dissimilar alloys. *Hot Work. Technol.* **2014**, *41*, 153–155.
27. Zhang, Z.K.; Wang, X.J.; Wang, P.C.; Zhao, G. Friction stir keyholeless spot welding of AZ31 Mg alloy-mild steel. *Trans. Nonferr. Met. Soc. China* **2014**, *24*, 1709–1716. [CrossRef]
28. Shiri, S.G.; Sarani, A.; Hosseini, S.R.E.; Roudini, G. Diffusion in FSW joints by inserting the metallic foils. *J. Mater. Sci. Technol.* **2013**, *29*, 1091–1095. [CrossRef]
29. Shi, H.; Chen, K.; Liang, Z.; Dong, F.; Yu, T.; Dong, X.; Zhang, L.; Shan, A. Intermetallic compounds in the banded structure and their effect on mechanical properties of Al/Mg dissimilar friction stir welding joints. *J. Mater. Sci. Technol.* **2017**, *33*, 359–366. [CrossRef]
30. Ji, S.D.; Jin, Y.Y.; Yue, Y.M.; Gao, S.S.; Huang, Y.X.; Wang, L. Effect of temperature on material transfer behavior at different stages of friction stir welded 7075–T6 aluminum alloy. *J. Mater. Sci. Technol.* **2013**, *29*, 955–960. [CrossRef]